Research Square

Preprints are preliminary reports that have not undergone peer review.
They should not be considered conclusive, used to inform clinical practice,
or referenced by the media as validated information.

Light-dependent reversible biofilm formation in the model cyanobacterium Synechocystis sp. PCC 6803

Mariann Kis

kis.mariann@blki.hun-ren.hu

HUN-REN Balaton Limnological Research Institute

Attila W. Kovács

HUN-REN Balaton Limnological Research Institute

Gábor Bernát

HUN-REN Balaton Limnological Research Institute

Research Article

Keywords: cyanobacterial biofilm, cell aggregates formation, DIC microscopy, EPS determination, log-normal distribution, PSII photochemistry

Posted Date: April 2nd, 2026

DOI: https://doi.org/10.21203/rs.3.rs-9177140/v1

License: This work is licensed under a Creative Commons Attribution 4.0 International License.
Read Full License

Additional Declarations: No competing interests reported.

Abstract

In response to light regime changes, the model cyanobacterium *Synechocystis* sp. PCC 6803 can switch from a planktonic lifestyle to form a phototrophic biofilm. Its planktonic cultures contain single cells and microcolonies, while the formed biofilms are dominated by cell aggregates with remarkable heterogeneity. We fitted the size distribution of the latter with a log-normal function and found that under low-to-moderate light intensities (<100 μmol photons m^{-2} s^{-1}) as well as under yellow-orange (560-590 nm) monochromatic illumination the *Synechocystis* biofilms are dominated by small aggregates with 10-15 μm^2 mean aggregate area, while higher (250-400 μmol photons m^{-2} s^{-1}) light intensities and blue-to-green (460–510 nm) illumination induced broad distribution function curves with 40-50 μm^2 mean aggregate area. The determined extracellular polymeric substance (EPS) concentrations were significantly higher in biofilm cultures (~1-3 μg/mL) compared to planktonic ones (<1 μg/mL) under the applied light intensities. In biofilms, violet-to-green (430-540 nm) monochromatic illumination induced the highest (~3-7 μg/mL) observed EPS concentrations, while yellow-orange illumination induced only ~0.5 μg/mL EPS levels, the same as in planktonic cultures, regardless the applied light regime. Growth rates and EPS production showed the opposite pattern: cultures grown under 630 nm light exhibited the highest growth rates and minimal EPS secretion, while cultures grown under 460 nm light showed the lowest growth rate and maximal EPS secretion. The chlorophyll fluorescence parameters derived from OJIP curves revealed that biofilm-associated cells had a smaller pool size of electron acceptors (S_M), a reduced maximum photochemical efficiency (φP_0), an increased apparent antenna size of PSII (ABS/RC), and an enhanced energy dissipation (DI_0/RC) relative to planktonic cells.

Introduction

One of the widely studied microorganisms, the cyanobacterium *Synechocystis sp*. PCC 6803 (hereafter referred as *Synechocystis*; Kaneko et al., 1996; Ikeuchi and Tabata, 2001) is widely used in laboratory experiments including studying photosynthetic electron transport, stress acclimation, redox regulation, as well as carbon and nitrogen metabolism (Allen, 2014; Burnap et al., 2015). Beside these, *Synechocystis* have also been used as a model organism in studying microbial connectivity and surface-associated lifestyles. Despite its unicellular nature, it readily forms aggregates, flocculated forms, and surface-adherent biofilms under various laboratory and environmental conditions (Jittawuttipoka et al., 2013; Allen et al., 2019).

Some microorganisms often switch between free-living planktonic state and surface-associated biofilm lifestyle; such a transition strongly alters cellular physiology, gene expression pattern, and ecological performance (Costerton et al., 1995; Flemming and Wingender, 2010). Biofilms are structured microbial communities embedded in an extracellular polymer produced by the cells and then either attached to biotic or abiotic surfaces or exist as aggregates. Phototrophic biofilms develop gradients (according to light, oxygen, inorganic carbon and nutrient availability), resulting in heterogeneity in cellular metabolism, growth and division (Stal, 1995; de Beer et al., 1997). In *Synechocystis*, the transition between planktonic

growth and biofilm formation can be triggered by environmental changes such as light conditions, nutrient availability, ionic strength and surface properties (Jittawuttipoka et al., 2013; Allen et al., 2019). Cellular cilia, cell wall proteins and the produced extracellular polymer trigger cell-to-cell cohesion and surface adhesion (Bhaya et al., 2002; Fisher et al., 2013).

A fundamental element of biofilms is the extracellular polymeric substance (EPS), which, together with the cells, creates a matrix that provides stability and a boundary between the cells and their environment (Flemming and Wingender, 2010). EPS produced by cyanobacteria is predominantly composed of polysaccharides and often contains proteins, nucleic acids and lipids (De Philippis et al., 2001; Pereira et al., 2015). EPS also protects cells from desiccation and freezing, participates in the diffusion and storage of gases and nutrients, and provides protection against high light intensity and oxidative stress through its structural features (De Philippis and Vincenzini, 1998; Tamaru et al., 2005).

Microbial biofilms are structurally heterogeneous both in natural and laboratory-controlled conditions. They contain single cells, dividing cells, microcolonies, and clusters of cells with various sizes and shapes. Due to the high degree of variability, the size distribution of these aggregates usually does not follow normal distribution. Rather, among different distribution functions, the cluster size distribution of biofilms can often be described with log-normal functions (Hirano et al., 1982; Tsagkari et al., 2022). Although several multiplicative processes (growth, adhesion, detachment, merge of aggregates) occur during biofilm formation, log-normal distribution is well suited to describe both natural and laboratory-grown biofilm structures. Parameters derived from the corresponding fits (e.g. mean (μ) and variance (σ)) both characterize cluster size distribution and the extent of structural heterogeneity, thereby enabling comparisons between different laboratory treatments or environmental conditions.

Light, besides being the primary energy source of phototrophic organisms (and thus the entire food web), is also the most important environmental factor that regulates photosynthesis and growth. In the case of biofilms light has also a major role in community organization. Light intensity directly controls the rate of photosynthesis, adjusts redox balance and nutrient distribution, and regulates the formation of a biofilm matrix, while high light intensities may cause photoinhibition and oxidative stress (Murata et al., 2007; Hihara et al., 2001). In biofilms, outer cells provide shading for the inner ones and the EPS matrix itself scatters light. These together create vertical light gradients and microscopic domains with different physiological states (Stal, 1995; Kühl et al., 1997). In addition to light intensity, light quality also varies within the biofilms. In natural environments, where microbial mats and benthic biofilms are common, spectral filtering results in wavelength-dependent niches, potentially promoting aggregation and biofilm formation as strategies to optimize light harvesting and photoprotection (Sand-Jensen, 2014; Helbling et al., 2015).

This work combines multi-intensity and multi-wavelength light treatments with biofilm-specific measurements to obtain information on the biofilm formation of *Synechocystis*, revealing some physiological and photobiological features not observed in planktonic cultures.

In this work, we study the planktonic *vs.* biofilm lifestyle, reversible biofilm shaping, aggregate formation, EPS production, and photosystem II (PSII) photochemistry of the unicellular cyanobacterium *Synechocystis* sp. PCC 6803 over the photon flux density (PFD) range of 10–400 μmol photons m^{-2} s^{-1} and the entire photosynthetically active radiation (PAR) spectrum, from 430 nm to 690 nm. We systematically analyzed differential interference contrast micrographs from planktonic and biofilm cultures grown under different light regimes. These micrographs were subsequently used for quantitative morphometric analysis (log-normal distribution of aggregates) and EPS determination (*via* colorimetric assay) under different treatments. Besides, we systematically compared OJIP fluorescence parameters between planktonic and biofilm *Synechocystis* cultures.

Materials and Methods

Strain and cultivation: *Synechocystis* sp. PCC 6803 cells were grown in Erlenmeyer flasks at constant 24°C in liquid BG-11 medium (Stanier et al. 1971) in an algae culture room. The stock cultures were cultivated under warm-white fluorescent lamps providing photon flux density of 25 μmol photons m^{-2} s^{-1}. The flasks with planktonic (suspended, non-biofilm) cultures were placed on an orbital shaker (50 rpm) with glass beads (diameter: 2–3 mm) inside, which kept suspension homogeneity, while the biofilm cultures were left undisturbed (i.e. unshaken and without beads) on the cultivation bench until sampling. During the light quantity acclimation experiments, the cultures were illuminated with diffuse warm-white light with intensities of 10, 25, 50, 100, 250, and 400 μmol photons m^{-2} s^{-1}. Under the light quality acclimation experiments, the cultures were illuminated by monochromatic light emitting diodes (LEDs) with nine different peak wavelengths (430, 460, 510, 540, 560, 590, 630, 660, and 690 nm) under the same PFD of 25 μmol photons m^{-2} s^{-1}. Illumination was provided as diffuse light from underneath the flasks using a home-built cultivation apparatus (Bernát et al. 2021; Zavřel et al. 2024). The light regime was set to 16h:8h (light:dark) and the cultures were grown to late-exponential phase (OD_{750} = 0.7–0.8), with active cell division and biofilm formation.

Differential Interference Contrast (DIC) microscopy

The different phases of cellular growth, aggregation development, and biofilm formation of *Synechocystis* under different light regimes were tracked by light microscopy. Prior to and during the sampling, the cultures were gently handled to avoid damaging the biofilm structure. The cells were fixed with 4% glutaraldehyde. 20 μL aliquot of a well-mixed sample was pipetted onto a microscope slide and covered by a cover plate (20 × 20 mm). DIC images were recorded using an Olympus BX51 microscope with a Differential Interference Contrast optical configuration equipped with a high performance DP75 digital microscope camera (Olympus). Twenty randomly selected parts of the field of view were recorded per each sample. Images were captured using an Olympus cellSens Dimension software (version 4.2.1) in grayscale mode to enhance structural contrast at a resolution of 2048 × 1500 pixels. Altogether, in each image about 200–400 objects were detected and used for quantifying morphological parameters.

Determination of the aggregate areas: Aggregate areas on DIC images were determined using the FIJI/ImageJ open-source Java-based image processing software (version 1.46r) (Schindelin et al. 2012.). Prior to the analysis, the spatial scale was set to 2.9 pixels per μm for all images, according to the microscope setup. To minimize user preconception and maximize reproducibility, an ImageJ macro set was written to automate object analysis (see Supplementary text). The steps of the workflow were as follows: (1) conversion images to 8-bit, (2) thresholding and masking, (3) hole-filling and watershed, and (4) particle analysis. Besides, the macro included minimum (3 μm²) and maximum (3000 μm²) object size in order to exclude cell debris and extremely large, biologically irrelevant, fused aggregates from the analysis.

Log-Normal Distribution model

To determine the size distribution of the cellular aggregates, we evaluated the calculated area data (see above) using a log-normal distribution model. Approximately 1000 to 3000 objects (i.e. single cells, microcolonies, and aggregates) were initially detected from the images obtained from each treatment. Small objects corresponding to single cells (~ 3 μm²) and microcolonies (3–5 cells) were excluded from further analysis using a lower cutoff of ≥ 10 μm² (Rochex and Lebeault 2007). We also used percentile trimming (lower 95%) to remove large outliers (i.e. merged clusters). The remaining 200 to 600 objects per treatment were used for fitting a log-normal distribution. This fitting resulted in cumulative distribution function (CDF) curves, as well as mean values (μ), standard deviation (σ), and shape parameters in log-space. The arithmetic mean in linear-space was back-transformed using standard expression ($\exp(\mu + \sigma^2/2)$) for the log-normal distribution. These parameters were used to compare aggregate size characteristics of cultures grown under different light regimes.

EPS isolation from Synechocystis cultures: The isolation procedure accounts for EPS dissolved in the growth medium as well EPS bound to the cells. From each Erlenmayer flask, 1 mL homogenous cell suspension was aliquoted and centrifuged at 5000 *g* for 10 min at 4°C. The remaining supernatant contained soluble EPS. The pellet was then resuspended in Tris-HCl (pH: 7.5, 10 mM) and shaken (100 rpm) at room temperature for 60 min to release bound EPS (Keithley and Kirisits 2018). The subsequent centrifugation (6000 *g*, 15 min, 4°C) was to separate solubilized EPS from the cells. The collected supernatants (containing the soluble and released EPS, respectively) were used for EPS determination using a colorimetric assay (see below). The pellets containing intact EPS-free cells were resuspended in 1 mL BG-11 medium and the corresponding OD_{750} values were measured using a double-beam spectrophotometer (Specord 210 Plus, Analytik Jena, Jena, Germany) as a proxy for biomass.

Colorimetric assay for EPS determination: As EPS is mostly composed of polysaccharides (exo-polysaccharides), colorimetric methods for carbohydrate determination are a suitable approach for EPS determination. EPS content of the obtained supernatants (see above) was precipitated with 100% ice-cold ethanol (1:1) and incubated overnight at 4°C. After the ethanol treatment, the samples were dried out at 40–45°C, followed by a rapid addition of the reagent solution of 200 μL sterile distilled water, 200 μL 5% phenol, and 1 mL concentrated sulfuric acid (Dubois et al. 1956, Kis et al. 2018). After waiting 10

min for color development in the dark and cooling in a water bath at 22°C, optical density was determined by a double-beam Specord 210 Plus spectrophotometer at 490 nm. For quantitative assessment of the EPS content, this colorimetric method was calibrated by a series of glucose solutions of known concentrations (0, 2, 5, 10, 20 µg/mL). To avoid any possible interference with other substances different from glucose, corrections were made by running a parallel assay without adding phenol.

PSII photochemistry: Rapid chlorophyll fluorescence induction (OJIP) curves of light-acclimated cultures were recorded using an AquaPen (Photon System Instruments, Brno, Czechia) with applying 620 nm saturation pulses of PFD 3000 µmol photons m^{-2} s^{-1}. From OJIP curves, the following parameters were retrieved: F_O, F_J, F_I and F_M, referring to the fluorescence yields at the O, J, I and P points of the OJIP curves, respectively. These parameters were used to calculate the maximum quantum yield, φP_O (= $F_V/F_M = (F_M-F_O)/F_M$) representing the maximum quantum yield of PSII, the normalized area, S_M (= Area/(F_M-F_O)) above the OJIP curve, being proportional with the pool size of electron acceptors of the photosynthetic electron transport chain, the apparent antenna size of an active PSII, ABS/RC, and the flux of energy dissipated in processes other than trapping per active PSII, DI_O/RC by the instrumental software. Fluorescence data were pre-processed by analytical tools available at https://tools-py.e-cyanobacterium.org/.

Results

DIC images of planktonic and biofilm cultures

To investigate how planktonic *vs*. biofilm growth influence the structural organization of *Synechocystis* cells, first we compared DIC microscopic images of cultures grown in planktonic form to those of biofilm cultures (Fig. 1). Planktonic cultures existed as highly dispersed cell suspensions, containing single cells and microcolonies only (Fig. 1A). In contrast, biofilm cultures exhibited a significantly different appearance, with a large number of cell aggregates with significant heterogeneity (Fig. 1B). In biofilm cultures, the aggregates ranged from small microcolonies of a few cells to large, compact clusters. This suggests that physiological conditions that induce biofilm formation also promote cell-to-cell adhesion and colony development. Thus, the presented images represent two distinct physiological states, i.e. planktonic lifestyle with single cells and microcolonies and a biofilm-forming, aggregated lifestyle.

Effect of light intensity on biofilm aggregates

We determined the area of a significant number of individual aggregates (200–600) formed under different PFDs (10–400 µmol photons m^{-2} s^{-1}) to explore how light intensity affect the development and aggregate size distribution of the biofilm. The resulting distributions showed clear differences between treatments (Fig. 2A). The cumulative distribution function (CDF) curves under low-to-moderate light intensities (10–100 µmol photons m^{-2} s^{-1}) showed the dominance of small aggregates and only minor

aggregate development. In contrast, a pronounced shift occurred at higher PFDs (250–400 µmol photons m^{-2} s^{-1}), showing the formation of larger aggregates (Fig. 2A).

This structural shift was supported by the corresponding values of the log-normal distribution parameters: µ and σ, respectively (Supplementary Fig. 1A). Both parameters showed a similar pattern with a minimum between 25 and 50 µmol photons m^{-2} s^{-1} PFDs, and a strong increase above 100 µmol photons m^{-2} s^{-1} growth light intensity. The increase in both µ (mean area) and σ (distribution broadening) reflect a shift towards larger aggregates.

The magnitude of these changes is best shown by the calculated mean aggregate areas (Fig. 2B). This showed small aggregate sizes (~ 15–20 μm^2) with only minor fluctuations between 10 and 100 µmol photons m^{-2} s^{-1} growth light intensities which increased up to 35 and 42 μm^2 under 250 and 400 µmol photons m^{-2} s^{-1} PFDs, respectively. This suggests that *Synechocystis* aggregate formation is enhanced by high irradiance.

Cultivation wavelength influences biofilm formation in Synechocystis

Compared to growth light intensity, cultivation wavelength influences aggregate size to a higher extent. *Synechocystis* cultures grown under monochromatic lights showed a strong spectral dependence in regards to aggregate size distribution (Fig. 2C). Biofilm cultures grown under violet-to-green lights (430–540 nm) were characterized by slowly rising CDF curves (with the highest effect at 460–510 nm) compared to that of cultures grown under longer wavelengths, indicating the formation of larger aggregates with remarkable size heterogeneity under violet-to-green lights.

In accordance, both µ and σ parameters (Supplementary Fig. 1B) and the mean area (Fig. 2D) peaked sharply at 460–510 nm. This indicates that growth under blue-green light cultivation promotes not only an increase in aggregate size (~ 45–50 μm^2) but also a robust broadening of size distribution, with a heterogeneous mixture of small to very large aggregates. Similarly to the mean area, the µ and σ parameters had the lowest values at 560 nm, with uniformly small (~ 12 μm^2) and narrowly distributed aggregates.

Light quantity and spectral quality strongly determine EPS production in Synechocystis

We determined total polysaccharide content in cultures as a proxy for polysaccharide-rich EPS level to investigate how light regimes (i.e. different light intensities and cultivation wavelengths) affect the secretion of EPS in *Synechocystis* (Fig. 3). EPS concentrations were significantly higher in biofilm cultures (~ 1–3 µg/mL) compared to planktonic ones (< 1 µg/mL), confirming that EPS secretion is closely related to cellular adhesion.

Over the applied PFD range, the EPS concentration of biofilm cultures showed its minimum level under 25 µmol photons m^{-2} s^{-1} growth light (Fig. 3A, black), in good accordance with the observation that this culture produced the smallest and least heterogeneous aggregates (Fig. 2A–B). At lower and higher PFDs, the EPS concentration was higher reaching its maximum (~ 3 µg/ml) in cultures grown under

white light with an intensity of 400 µmol photons m^{-2} s^{-1}. EPS concentration in planktonic cultures was also tested and it remained low through all studied light intensities (Fig. 3A, red), suggesting that EPS excretion is closely related to the biofilm-associated lifestyle rather than a bulk cellular property. This contrasts to growth rates, which are essentially higher in planktonic cultures than in biofilms.

EPS production in *Synechocystis* biofilm cultures was more sensitive to cultivation wavelength than to light intensity (Fig. 3B). Under constant PFDs of 25 µmol photons m^{-2} s^{-1}, violet-to-green monochromatic illumination (430–540 nm) induced the highest EPS levels (~ 3–7 µg/mL), far more to all other wavelengths (~ 0.5–1.5 µg/mL). EPS content had its minimal values (~ 0.5 µg/mL, similar to the planktonic levels (Fig. 3A)) under yellow-orange wavelengths (560–590 nm). This wavelength dependence is very similar to that of aggregate size (Fig. 2D), indicating that blue light promotes EPS biosynthesis and, in turn, increases aggregate size and heterogeneity.

EPS production under changing light regime

Figure 4 shows how EPS production responds to changing light regime. During pre-cultivation under warm-white light (A) and, subsequently, under red (630 nm) cultivation light (B), EPS content remained low (~ 1 µg/mL). However, upon a transfer to 460 nm light (C), EPS concentration increased rapidly and continuously, reaching the highest observed value in our study. When cultures were replaced under red light after a dilution (D, B), EPS concentration returned to the original level. As we have shown previously (Zavřel et al. 2024), *Synechocystis* cultures grown under 630 nm and 460 nm lights have the highest and lowest growth rates, respectively, among the nine tested wavelengths, the opposite of what we observed with EPS secretion. This suggests that EPS production is not a passive accompanying phenomenon of growth, rather, is an actively regulated photo-physiological response.

PSII photochemistry in planktonic and biofilm cells

We determined several chlorophyll fluorescence parameters (derived from OJIP curves, see Materials and Methods) in both planktonic and biofilm *Synechocystis* cultures over a range of PFDs (Fig. 5). We used these parameters to characterize PSII photochemistry, electron transport capacity and energy dissipation in these cultures.

The light dependence of the normalized area above the OJIP transient (S_M) showed entirely different patterns in the two growth modes (Fig. 5A). In planktonic cells, S_M reached a maximum under 25 µmol photons m^{-2} s^{-1} PFD and decreased gradually with increasing light intensities. In contrast, biofilm cells showed high S_M values only under 10 µmol photons m^{-2} s^{-1} growth light and under other intensities, S_M values remained low. This indicates a reduced electron acceptor capacity in biofilm cultures under elevated irradiance.

The maximum quantum yield of PSII photochemistry decreased with increasing intensities in both planktonic and biofilm cells (Fig. 5B). The obtained φP_0 values (~ 0.3–0.4) were statistically indifferent between the two life forms under low-to-moderate light intensities. However, biofilm cells showed

significantly lower values (~ 0.12) compared to the planktonic ones (~ 0.22) at the highest applied irradiance. This suggests a more effective electron transport in planktonic *Synechocystis* cells than that of biofilm ones under high light intensities.

This conclusion is well supported by DI_0/RC data. This flux of dissipated energy increased gradually in biofilm cells with increasing PFDs (Fig. 5C). However, while planktonic cells showed only a moderate increase and fluctuation, biofilm cells displayed a much steeper rise under high light intensities, indicating an enhanced energy dissipation under high light conditions.

The antenna size of an active PSII, ABS/RC values also increased with increasing PFDs in both planktonic and biofilm cells (Fig. 5D). However, biofilm cells showed higher ABS/RC values compared to planktonic ones at irradiances above 100 µmol photons m^{-2} s^{-1} PFD. The difference becomes significant above 250 µmol photons m^{-2} s^{-1} PFD, indicating a higher absorption cross section per active reaction center in the biofilm cultures.

Discussion

Our results with planktonic and biofilm *Synechocystis* cultures show a light-dependent structural and physiological changes between unicellular organization and biofilm lifestyle. While planktonic cultures are predominantly unicellular, biofilm cultures consist of aggregates with a broad spectrum of size distribution, ranging from microcolonies of a few cells to large, compact clusters. Aggregate formation suggests that *Synechocystis* cells in a biofilm switched to a physiological state that promotes cell-to-cell adhesion and matrix formation, rather than representing passive sedimentation and surface-associated phenomena (Fisher et al., 2013; Jittawuttipoka et al., 2013; Enomoto et al., 2015). Biofilm-associated aggregation has been described previously in *Synechocystis* and other cyanobacteria. The observed aggregation is a consequence of an enhanced EPS production, which changes the cell surface properties and, in turn, increases their adhesive capacity (Fisher et al., 2013; Enomoto et al., 2015). The transition from unicellular to colonial organization has also been observed in *Microcystis*, *Nostoc*, and *Anabaena* species, where aggregation is an advantage in terms of enhanced stress tolerance and environmental resistance (De Philippis et al., 2001; Gan et al., 2012.; Sand-Jensen, 2014). Our observations based on microscopic imaging (Fig. 1) and subsequent quantitative analyses of aggregate size (Fig. 2), as well as the determined EPS level (Figs. 3, 4) and photosynthetic parameters (Figs. 5) clearly confirm that the biofilm lifestyle fundamentally differs from the planktonic one.

Quantitative analysis of the size distribution of cellular clusters revealed that light intensity largely influences the size and heterogeneity of *Synechocystis* aggregates (Fig. 2A–B). Under moderate PFDs *Synechocystis* biofilms are dominated by relatively small, narrowly distributed aggregates, while low and high PFDs induce the formation of larger clusters with great structural heterogeneity.In cyanobacterial biofilms, EPS production is an essential element of cell-to-cell adhesion, aggregate development and expansion (De Philippis et al., 1998; Seminara et al. 2012). The similarity between the light-intensity-dependence of aggregate size (Fig. 2B) and EPS secretion (Fig. 3A) confirms that both low and, in

particular, high irradiance facilitates EPS-mediated cellular adhesions. Sub-optimal light environment may trigger protective responses including increased production of EPS, which can act as a physical barrier between cell surface and environment as well as the appearance of larger, heterogeneous aggregates (at higher PFDs) to protect cells against photodamage *via* self-shading (Pereira et al., 2009; Rossi and De Philippis 2015).

Compared to light intensity, growth wavelength had an even more pronounced influence on aggregate size and heterogeneity in *Synechocystis* biofilms (Fig. 2C–D). Blue and blue-green growth lights induce the formation of remarkably large, heterogeneous aggregates, whereas the growth under yellow-orange light promotes the formation of uniformly small structures, similar to planktonic cultures. Growth under near far-red light (690 nm) implied intermediate aggregation. This wavelength dependent phenomenon strongly suggests the involvement of blue-light specific signaling pathways rather than energetic effects. In *Synechocystis*, several blue-light photoreceptors and cryptochrome-like proteins regulate cellular behavior, including phototaxis and type IV pili–dependent motility, stress responses, and gene expression (Masuda and Bauer, 2002; Song et al., 2011.; Wiltbank and Kehoe, 2019; Sugimoto et al. 2017). In cyanobacteria and other phototrophs, blue light enhances EPS accumulation and cellular-surface attachment, often independently of growth rate (Ikeuchi and Ishizuka, 2008; Enomoto et al., 2015).

The strong wavelength dependence of aggregate dynamics (Fig. 2C–D) correlates well with that of EPS production (Fig. 3B). Based on research by Luimstra et al. (2018), blue light (~ 450 nm) has a significant negative effect on the growth of the *Synechocystis* cells compared to red or white light. Blue light induces the development of extracellular matrix formation, creating a physical barrier to protect cells against excess excitation energy in the heterogeneous biofilm structures. In contrast, orange-red light is effectively absorbed and utilized in *Synechocystis* inducing rapid growth (Zavřel et al. 2024) and low EPS production, and induces a planktonic-like physiological state, since under optimal conditions, protection and biofilm formation are not necessary.

The EPS secretion in biofilm cultures changes dynamically, depending on light regime. EPS determination under changing environmental (light) conditions (Fig. 4) demonstrates that EPS production in biofilm cultures is actively regulated (De Philippis et al., 2001.; Ehling-Schulz et al., 1997). Upon switching from red to blue growth light, cellular growth significantly slowed down, accompanied by an enhanced (Zavřel et al. 2024, this work). This completely opposite wavelength dependence of cell growth and EPS secretion suggests the latter is an active regulatory process, rather than a passive secretation by cell proliferation (Gan et al., 2012.; Otero and Vincenzini, 2003). Similar inverse effects were found also in *Nostoc sp.* and *Microcystis sp.* strains, where EPS production was increased under stress or sub-optimal growth conditions (De Philippis et al., 2001; Gan et al., 2012). This reversibility suggests a remarkable physiological plasticity of *Synechocystis* cells under changing environmental conditions.

Biofilm-associated cells showed a reduced pool size of electron acceptors (S_M) over almost the entire range of light intensities (Fig. 5A), as well as lower maximum photochemical efficiency (φP_0), enhanced energy dissipation (DI_0/RC), and enlarged apparent antenna size (ABS/RC) under high light compared to planktonic cells (Fig. 5B–D). All of these changes are characteristic for photoprotective acclimations (Strasser et al., 2004.; Campbell et al., 1998.; Hendrickson et al., 2005). Concomitant increase of ABS/RC and DI_0/RC suggests that the higher excitation pressure per active PSII is compensated by an enhanced dissipation of excess energy as heat or fluorescence (Al-Najjar et al. 2010) in biofilm cells. Reduced S_M values further indicate a limitation on downstream electron transport, which may serve to prevent over-reduction of the photosynthetic electron transport chain (especially the plastoquinone pool) under higher light (Strasser et al., 2004). These photochemical features concur to the conditions promoting large aggregate formation and EPS accumulation (Figs. 2–3). Biofilms and mats modify the local light environment *via* light scattering and absorption, potentially increasing excitation heterogeneity within aggregates (Kühl 2005; Al-Najjar et al. 2010).

Conclusion

Our results demonstrated that both light quantity and quality strongly influence aggregate formation, EPS production, and photosynthetic efficiency in *Synechocystis* sp. PCC 6803. This coordinated performance highlights the close interrelationship between cellular growth and protection. This plausibility seems to be critical for survival in ever changing aquatic and benthic environments. The obtained data provide a deeper insight into cyanobacterial ecology and have potential relevance for various biotechnological applications including biofilm engineering.

Declarations

Data availability statement

All data and material are available upon request of the corresponding author. Additionally, we provide a freely accessible online tool for streamlined processing and preliminary analysis of fluorescence data from kinetic fluorometers and spectrofluorometers used in this study, available at https://tools-py.e-cyanobacterium.org/.

Declaration of competing interest

The authors declare that they have no known competing financial interests or personal relationships that could have appeared to influence the work reported in this paper.

Author contribution statement

MK designed the experiments. MK and AWK performed experiments. MK analysed the results. MK and GB wrote the manuscript. All authors reviewed, revised and approved the final manuscript for publication.

Funding

This work has been implemented by the National Multidisciplinary Laboratory for Climate Change (RRF-2.3.1-21-2022-00014) project within the framework of Hungary's National Recovery and Resilience Plan supported by the Recovery and Resilience Facility of the European Union.

References

1. Al-Najjar, M., de Beer, D., Jørgensen, B., Kühl M., Polerecky L. Conversion and conservation of light energy in a photosynthetic microbial mat ecosystem. *ISME J* 4, 440–449 (2010). https://doi.org/10.1038/ismej.2009.121
2. Allen, R., Rittmann, B. E., and Curtiss, R. III (2019). Axenic biofilm formation and aggregation by *Synechocystis* sp. strain PCC 6803 are induced by changes in nutrient concentration and require cell surface structures. *Applied and Environmental Microbiology*, 85(7), e02192-18. https://doi.org/10.1128/AEM.02192-18
3. Bernát, G., Zavřel, T., Kotabová, E., Kovács, L., Steinbach, G., Vörös, L., Prášil, O., Somogyi, B., Tóth, V. R. (2021). Photomorphogenesis in the Picocyanobacterium *Cyanobium gracile* Includes Increased Phycobilisome Abundance Under Blue Light, Phycobilisome Decoupling Under Near Far-Red Light, and Wavelength-Specific Photoprotective Strategies. *Frontiers in Plant Science*, 12, 612302. doi: 10.3389/fpls.2021.612302.
4. Bhaya, D., Bianco, N. R., Bryant, D., and Grossman, A. (2002). Type IV pilus biogenesis and motility in the cyanobacterium *Synechocystis* sp. PCC6803. *Molecular Microbiology*, 37, 941–951. https://doi.org/10.1046/j.1365-2958.2000.02068.x
5. Burnap, R. L., Hagemann, M., and Kaplan, A. (2015). Regulation of CO_2 concentrating mechanisms in cyanobacteria. *Life*, 5, 348–371. https://doi.org/10.3390/life5010348
6. Campbell, D., Hurry, V., Clarke, A. K., Gustafsson, P., and Öquist, G. (1998). Chlorophyll fluorescence analysis of cyanobacterial photosynthesis and acclimation. *Microbiology and Molecular Biology Reviews*, 62(3), 667–683. doi: 10.1128/MMBR.62.3.667-683.1998.
7. Costerton, J. W., Lewandowski, Z., Caldwell, D. E., Korber, D. R., and Lappin-Scott, H. M. (1995). Microbial biofilms. *Annual Review of Microbiology*, 49, 711–745. https://doi.org/10.1146/annurev.mi.49.100195.003431
8. de Beer, D., Stoodley, P., Roe, F., and Lewandowski, Z. (1997). Effects of biofilm structures on oxygen distribution and mass transport. *Biotechnology and Bioengineering*, 43(11) 1131-8. doi: 10.1002/bit.260431118.
9. De Philippis, R., and Vincenzini, M. (1998). Exocellular polysaccharides from cyanobacteria and their possible applications. *FEMS Microbiology Reviews*, 22, 151–175. https://doi.org/10.1111/j.1574-6976.1998.tb00365.x

10. De Philippis, R., Sili, C., Paperi, R., and Vincenzini, M. (2001). Exopolysaccharide-producing cyanobacteria and their possible exploitation: a review. *Journal of Applied Phycology*, 13, 293–299. https://doi.org/10.1023/A:1017590425924
11. DuBois, M., Gilles, K. A., Hamilton, J. K., Rebers, P. A., and Smith, F. (1956). Colorimetric method for determination of sugars and related substances. *Analytical Chemistry* 28(3):350–356. https://doi.org/10.1021/ac60111a017
12. Ehling-Schulz, M., Bilger, W., and Scherer, S. (1997). UV-B-induced synthesis of photoprotective pigments and extracellular polysaccharides in the terrestrial cyanobacterium *Nostoc commune*. *Journal of Bacteriology* 179: 1940–1945. doi: 10.1128/jb.179.6.1940-1945.1997.
13. Enomoto, G., Nomura, R., Shimada, T., Ni-Ni-Win, Narikawa, R., and Ikeuchi, M. (2014). Cyanobacteriochrome SesA is a diguanylate cyclase that induces cell aggregation in *Thermosynechococcus*. *Journal of Biological Chemistry*, 289(36), 24801–24809. doi: 10.1074/jbc.M114.583674
14. Enomoto, G., Ni-Ni-Win, Narikawa, R., and Ikeuchi, M. (2015). Three cyanobacteriochromes work together to form a light colour-sensitive input system for c-di-GMP signalling of cell aggregation. *Proceedings of the National Academy of Sciences USA*, 112(26), 8082–8087. DOI: 10.1073/pnas.1504228112
15. Fisher, M. L., Allen, R., Luo, Y., and Curtiss, R. III (2013). Export of extracellular polysaccharides modulates adherence of the cyanobacterium *Synechocystis*. *PLOS ONE*, 8(9), e74514. https://doi.org/10.1371/journal.pone.0074514
16. Flemming, H.-C., and Wingender, J. (2010). The biofilm matrix. *Nature Reviews Microbiology*, 8, 623–633.
https://doi.org/10.1038/nrmicro2415
17. Gan, N., Xiao, Y., Zhu, L., Wu, Z., Liu, J., Hu, C., and Song, L. (2012). The role of microcystins in maintaining colonies of bloom-forming *Microcystis* spp. *Environmental Microbiology*, 14(3), 730–742. https://doi.org/10.1111/j.1462-2920.2011.02624.x.
18. Gan, F., Zhang, S., Rockwell, N. C., Martin, S. S., Lagarias, J. C., and Bryant, D. A. (2014). Extensive remodeling of a cyanobacterial photosynthetic apparatus in far-red light. *Science*, 345, 1312–1317. https://doi.org/10.1126/science.1256963
19. Hagemann, M., and Hess, W. R. (2018). Systems and synthetic biology for the biotechnological application of cyanobacteria. *Current Opinion in Biotechnology*, 49, 94–99. https://doi.org/10.1016/j.copbio.2017.07.008
20. Helbling, E. W., Banaszak, A. T., and Villafañe, V. E. (2015). Global change feed-back inhibits cyanobacterial photosynthesis. *Scientific Reports*, 5, 14514. https://doi.org/10.1038/srep14514
21. Hendrickson, L., Forster, B., Pogson, B. J., and Chow, W. S. (2005). A simple chlorophyll fluorescence parameter that correlates with the rate coefficient of photoinactivation of Photosystem II. *Photosynthesis Research*, 84(1-3), 43–49. https://doi.org/10.1007/s11120-004-6430-4

22. Hihara Y, Sonoike K, Kanehisa M, Ikeuchi M. (2003) DNA microarray analysis of redox-responsive genes in the genome of the cyanobacterium Synechocystis sp. strain PCC 6803. *Journal of Bacteriology,* 185(5), 1719-25. doi: 10.1128/JB.185.5.1719-1725.2003.
23. Hirano SS, Nordheim EV, Arny DC, Upper CD.(1982) Lognormal Distribution of Epiphytic Bacterial Populations on Leaf Surfaces. *Applied and Environmental Microbiology*, 44(3) https://doi.org/10.1128/aem.44.3.695-700.1982
24. Ikeuchi, M., and Tabata, S. (2001). Synechocystis sp. PCC 6803—A useful tool in the study of the genetics of cyanobacteria. *Photosynthesis Research*, 70, 73–83. doi: 10.1023/A:1013887908680
25. Ikeuchi, M., and Ishizuka, T. (2008). Cyanobacteriochromes: a new superfamily of tetrapyrrole-binding photoreceptors in cyanobacteria. *Photochemical & Photobiological Sciences*, 7, 1159–1167. https://doi.org/10.1039/b802660m
26. Jittawuttipoka, T., Planchon, M., Spalla, O., Benzerara, K., Guyot, F., Cassier-Chauvat, C., and Chauvat, F. (2013). Multidisciplinary evidence that *Synechocystis* PCC 6803 exopolysaccharides operate in cell sedimentation and protection against salt and metal stresses. *PLOS ONE*, 8(2), e55564. https://doi.org/10.1371/journal.pone.0055564
27. Kaneko, T., Sato, S., Kotani, H., Tanaka, A., Asamizu, E., Nakamura, Y., Miyajima, N., Hirosawa, N., Sugiura, M., Sasamoto, S., Kimura, T., Hosouchi, T., Matsuno, A., Muraki, A., Nakazaki, A., Naruo, K., Okumura, S., Shimpo, S., Takeuchi, C., Wada, T., Watanabe, T., Yamada, M., Yasuda, M., and Tabata, S. (1996). Sequence analysis of the genome of the unicellular cyanobacterium *Synechocystis* sp. PCC 6803. *DNA Research*, 3, 109–136. https://doi.org/10.1093/dnares/3.3.109
28. Keithley S.A. and Kirisits M.J. (2018) An improved protocol for extracting extracellular polymeric substances from granular filter media. *Water Research*, 129,419-427. https://doi.org/10.1016/j.watres.2017.11.020
29. Kis, M., Sipka, G., Ayaydin, F., Maróti, P (2018). The biophysics of a critical phenomenon: colonization and sedimentation of the photosynthetic bacteria *Rubrivivax gelatinosus*. *European Biophysics Journal* 47, 139-149. https://doi.org/10.1007/s00249-017-1236-4
30. Kühl, M., Lassen, C., and Jørgensen, B.B. (1994) Light penetration and light intensity in sandy marine sediments measured with irradiance and scalar irradiance fiber-optic microprobes. *Marine Ecology Progress Series*, 105, 139–148. https://doi.org/10.3354/meps105139
31. Kühl, M. (2005). Optical microsensors for analysis of microbial communities. *Methods in Enzymology*, 397, 166–199. https://doi.org/10.1016/S0076-6879(05)97010-9
32. Luimstra V.M., Schuurmans J.M., Verschoor A.M., Hellingwerf K.J., Huisman J., Matthijs H.C.P. (2018) Blue light reduces photosynthetic efficiency of cyanobacteria through an imbalance between photosystems I and II. *Photosynthesis Research*, 138(2),177-189. doi: 10.1007/s11120-018-0561-5
33. Maeda, K., Okuda, Y., Enomoto, G., Watanabe, S., and Ikeuchi, M. (2021). Biosynthesis of a sulfated exopolysaccharide, synechan, and bloom formation in the model cyanobacterium *Synechocystis* sp.

PCC 6803. *eLife*, 10, e66538. https://doi.org/10.7554/eLife.66538

34. Masuda, S., and Bauer, C. E. (2002). AppA is a blue-light photoreceptor that antirepresses photosynthesis gene expression in *Rhodobacter sphaeroides*. *Cell*, 110(5), 613–623. https://doi.org/10.1016/S0092-8674(02)00876-0
35. Murata, N., Takahashi, S., Nishiyama, Y., and Allakhverdiev, S. I. (2007). Photoinhibition of photosystem II under environmental stress. *Biochimica et Biophysica Acta*, 1767, 414–421. https://doi.org/10.1016/j.bbabio.2006.11.019
36. Otero, A., and Vincenzini, M. (2003). Extracellular polysaccharide synthesis by *Nostoc* strains as affected by N source and light intensity. *Journal of Biotechnology,* 102, 143-152. https://doi.org/10.1016/S0168-1656(03)00022-1.
37. Paerl, H. W., and Pinckney, J. L. (1996). A mini-review of microbial consortia: their roles in aquatic production and biogeochemical cycling. *Microbial Ecology*, 31, 225–247. https://doi.org/10.1007/BF00171569
38. Pereira, S., Zille, A., Micheletti, E., Moradas-Ferreira, P., De Philippis, R., and Tamagnini, P. (2009). Complexity of cyanobacterial exopolysaccharides: composition, structures, inducing factors and putative genes. *FEMS Microbiology Reviews*, 33(5), 917–941. https://doi.org/10.1111/j.1574-6976.2009.00183.x
39. Pereira, S. B., Mota, R., Vieira, C. P., Vieira, J., Tamagnini, P., and De Philippis, R. (2015). Phylum-wide analysis of genes related to the assembly and export of extracellular polymeric substances in cyanobacteria. *Scientific Reports*, 5, 14835. https://doi.org/10.1038/srep14835
40. Rochex, A., and Lebeault, J.M., (2007) Effects of nutrients on biofilm formation and detachment of a *Pseudomonas putida* strain isolated from a paper machine, *Water Research*, 41(13), 2885–2892. https://doi.org/10.1016/j.watres.2007.03.041
41. Rossi F, De Philippis R. (2015) Role of cyanobacterial exopolysaccharides in phototrophic biofilms and in complex microbial mats. *Life (Basel)*. 5(2), 1218-38. doi: 10.3390/life5021218
42. Schindelin, J., Arganda-Carreras, I., Frise, E., Kaynig, V., Longair, M., Pietzsch, T., Preibisch, S., Rueden, C., Saalfeld, S., Schmid, B., Tinevez, J. Y., White, D. J., Hartenstein, V., Eliceiri, K., Tomancak, P., and Cardona, A. (2012). Fiji: an open-source platform for biological-image analysis. *Nature Methods*,. 9(7), 676-82. https://doi: 10.1038/nmeth.2019.
43. Song, J.-Y., Cho, H.-S., Cho, J.-I., Jeon, J.-S., Lagarias, J. C., and Park, Y.-I. (2011). Near-UV cyanobacteriochrome signaling system elicits negative phototaxis in the cyanobacterium *Synechocystis* sp. PCC 6803. *Proceedings of the National Academy of Sciences of the United States of America*, 108(26), 10780–10785. https://doi.org/10.1073/pnas.1104242108
44. Sugimoto Y., Nakamura H., Ren S., Hori K., Masuda S. (2017) Genetics of the Blue Light-Dependent Signal Cascade That Controls Phototaxis in the Cyanobacterium *Synechocystis* sp. PCC6803, *Plant and Cell Physiology*, 58(3), 458–465, https://doi.org/10.1093/pcp/pcw218

45. Stal, L. J. (1995). Physiology of cyanobacteria in microbial mats and other communities. *New Phytologist*, 131, 1–32. https://doi.org/10.1111/j.1469-8137.1995.tb03051.x
46. Stanier, R.Y., Kunisawa, R., Mandel, M., and Cohen-Bazire, G. (1971). Purification and properties of unicellular blue-green algae (order Chroococcales). *Bacteriology Reviews* 35:171–205. doi: 10.1128/br.35.2.171-205.1971
47. Strasser, R. J., Tsimilli-Michael, M., and Srivastava, A. (2004). Analysis of the chlorophyll a fluorescence transient. In G. C. Papageorgiou and Govindjee (Eds.), *Chlorophyll a Fluorescence: A Signature of Photosynthesis* (Advances in Photosynthesis and Respiration, 19, 321–362. Springer, Dordrecht. https://doi.org/10.1007/978-1-4020-3218-9_12
48. Tamaru, Y., Takani, Y., Yoshida, T., and Sakamoto, T. (2005). Crucial role of extracellular polysaccharides in desiccation and freezing tolerance in the terrestrial cyanobacterium *Nostoc commune*. *Applied and Environmental Microbiology*, 71, 7327–7333. https://doi.org/10.1128/AEM.71.11.7327-7333.2005
49. Tsagkari, E., Connelly, S., Liu, Z. *et al.* (2022) The role of shear dynamics in biofilm formation. *npj Biofilms Microbiomes* 8, 33. https://doi.org/10.1038/s41522-022-00300-4
50. Whitton, B. A., and Potts, M. (2012). *Ecology of Cyanobacteria II: Their Diversity in Space and Time*. Springer, Dordrecht. https://doi.org/10.1007/978-94-007-3855-3
51. Wilking, J. N., Angelini, T. E., Seminara, A., Brenner, M. P., and Weitz, D. A. (2011). Biofilms as complex fluids. *MRS Bulletin*, 36, 385–391. https://doi.org/10.1557/mrs.2011.71
52. Wiltbank, L. B., and Kehoe, D. M. (2019). Diverse light responses of cyanobacteria mediated by phytochrome-superfamily photoreceptors. *Nature Reviews Microbiology*, 17, 37–50. https://doi.org/10.1038/s41579-018-0110-4
53. Zavřel, T., Segečová, A., Kovács, L., Lukeš, M., Novák, Z., Pohland, A.-C., Szabó, M., Somogyi, B., Prášil, O., Červený, J. and Bernát, G. (2024). A Comprehensive Study of Light Quality Acclimation in *Synechocystis* Sp. PCC 6803. *Plant and Cell Physiology* 65, 1285-1297. https:/doi: 10.1093/pcp/pcae062

Figures

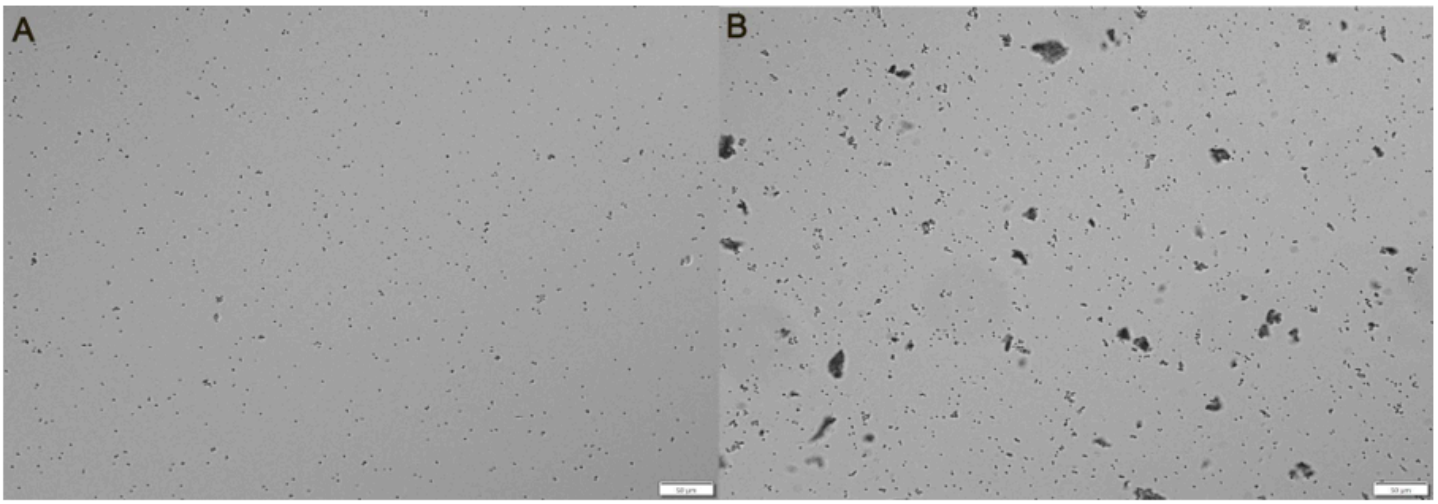


Figure 1

Differential interference contrast (DIC) micrographs of *Synechocystis* cultures grown in planktonic (A) or biofilm lifestyles (B). Scale bars: 50 µm.

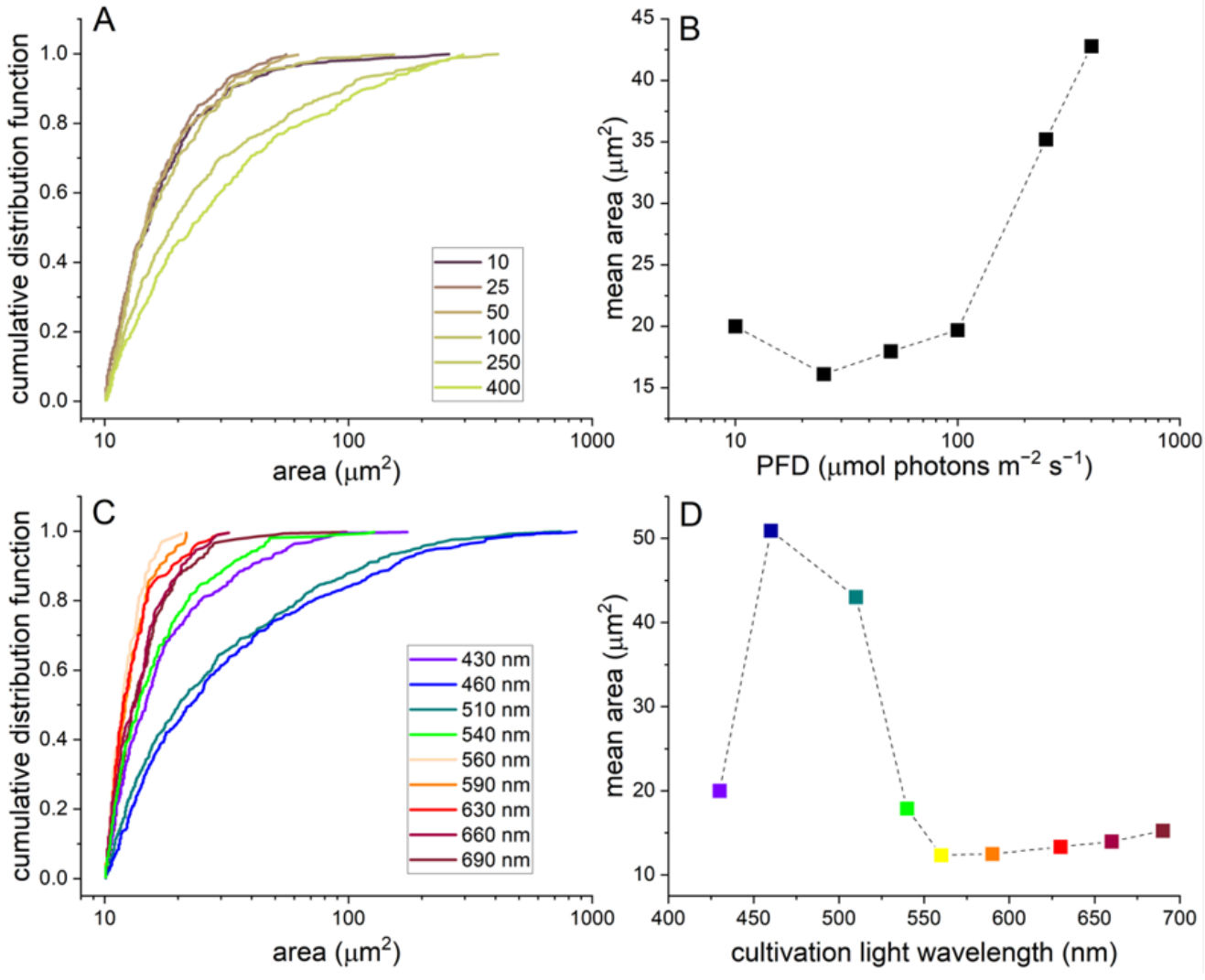


Figure 2

Log-normal size (area) distribution of *Synechocystis* biofilm aggregates developed under various photon flux densities (PFD) (A, B) and under nine different monochromatic lights (C, D). (A, C) Cumulative distribution function (CDF) curves of aggregate areas in biofilm cultures grown under various PFDs and monochromatic lights, respectively. (B, D) Mean aggregate areas in biofilm cultures grown under various PFDs and monochromatic lights, respectively.

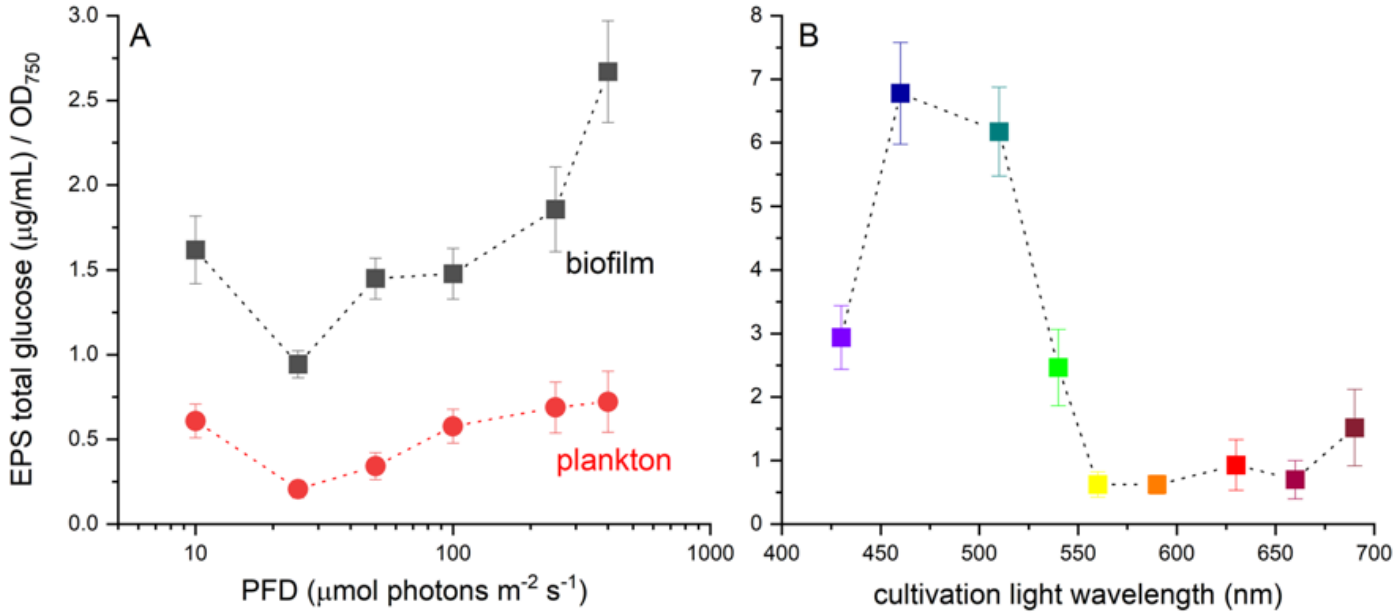


Figure 3

The level of extracellular polymeric substances (EPS), determined as total glucose concentration normalised to biomass (OD_{750}) in *Synechocystis* planktonic and biofilm cultures grown under different light regimes. (A, B) Total glucose equivalents (µg mL^{-1} OD_{750}^{-1}) as a proxy for EPS content in biofilm (A, B) and planktonic cultures (A), as a function of PFD (10–400 µmol photons m^{-2} s^{-1}) and growth wavelength at at a constant PFD of 25 µmol photons m^{-2} s^{-1}, respectively.

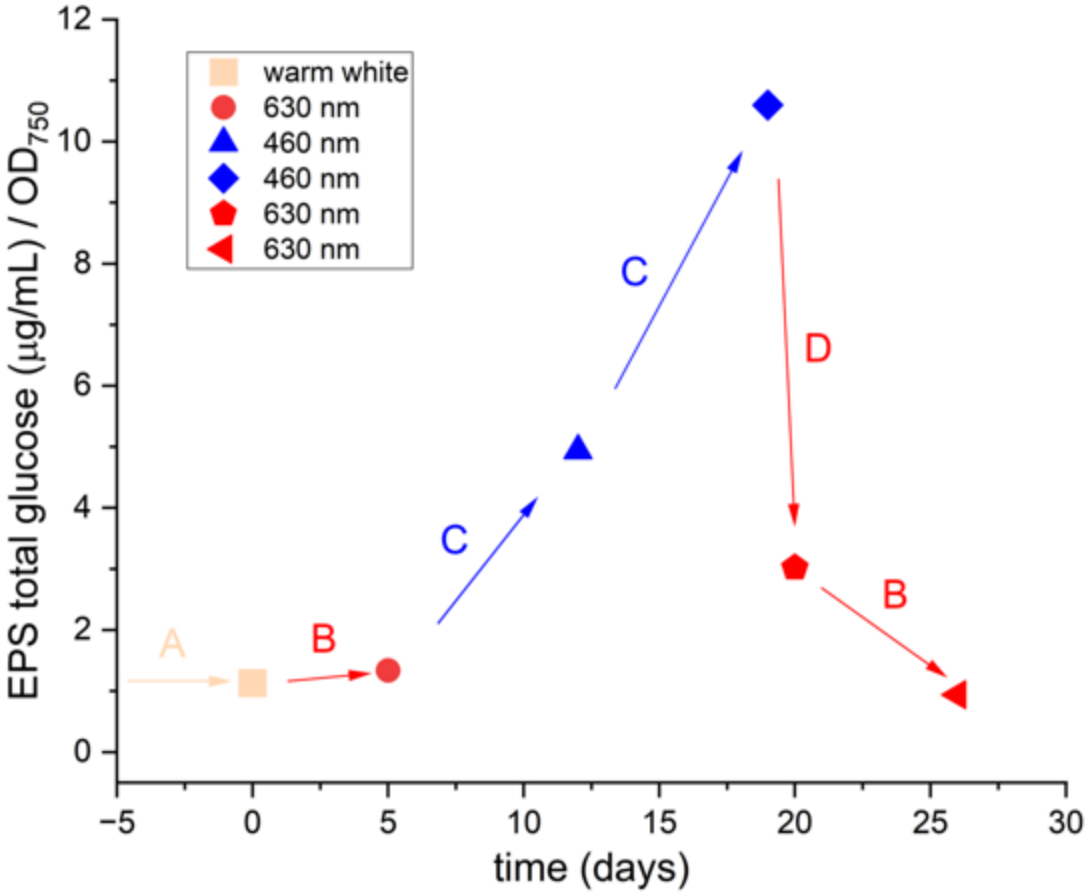


Figure 4

EPS production in *Synechocystis* under a changing light regime. EPS concentration (expressed as µg mL^{-1} glucose/OD_{750}) in a *Synechocystis*culture pre-cultivated under warm-white light for 5 days (A), followed by subsequent cultivations under 630 nm red light for 5 days (B), 460 nm blue light for 11 days (C), a 5-fold dilution (D) and a cultivation again under 630 nm red light. Light intensities at each step were set to 25 µmol photons m^{-2} s^{-1}. Arrows indicate the sequence of cultivation steps. Symbols denote individual sampling times at each cultivation phase.

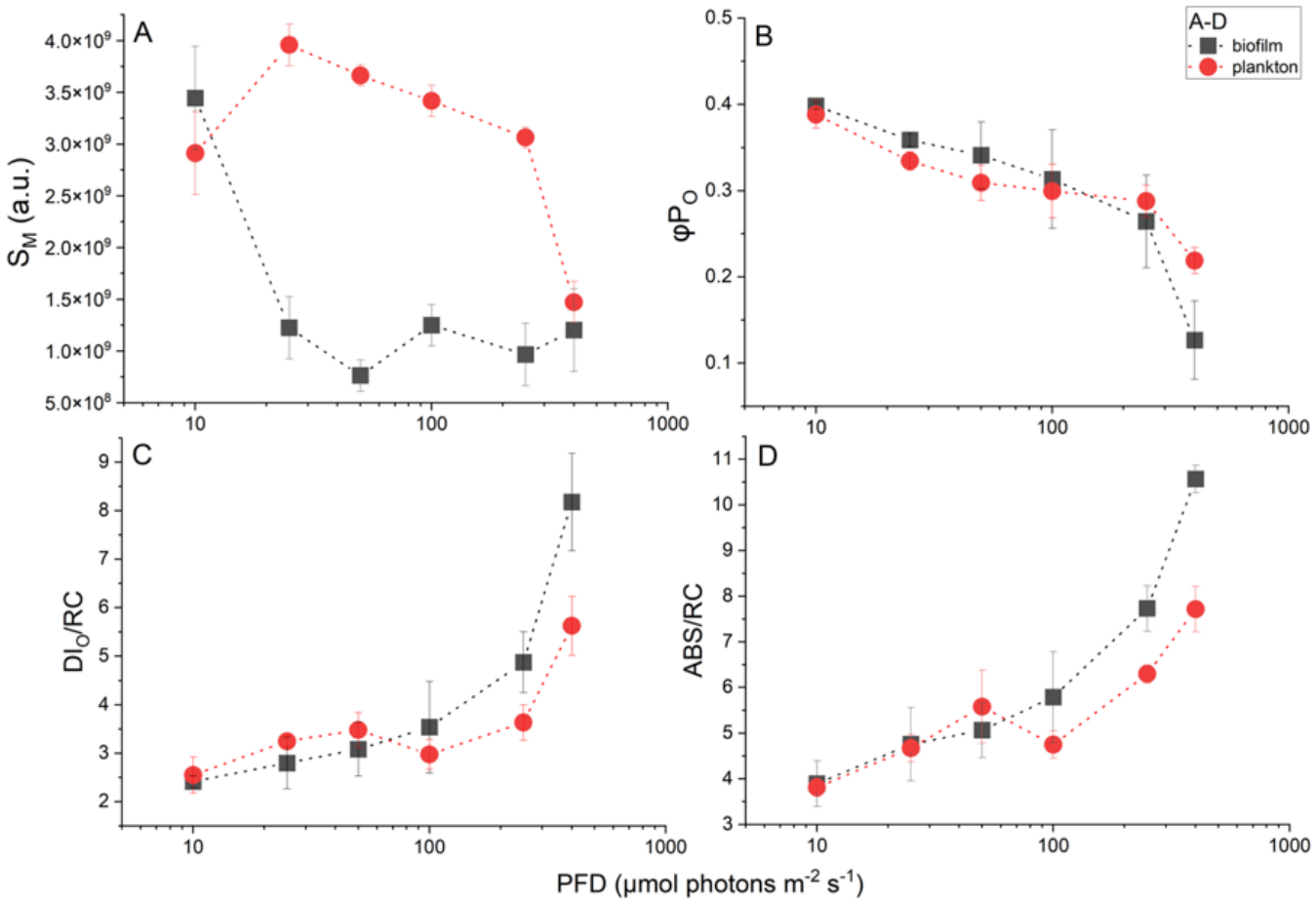


Figure 5

PSII photochemistry and energy fluxes in planktonic (red) and biofilm (black) *Synechocystis* cells under various growth light intensities. Chlorophyll fluorescence parameters were derived from fast fluorescence induction curves (OJIP) measured after dark acclimation. (A) S_M (Area/(F_M-F_O), normalized area above the OJIP curves, proportional to the pool size of electron acceptors of the photosynthetic electron transport chain. (B) Maximum quantum yield of PSII photochemistry (φP_O = (F_M - F_O) / F_M). (C) Apparent antenna size per active PSII reaction center (ABS/RC = (M_O/VJ)/φP_O). (D) Flux of energy dissipated in processes other than trapping per PSII reaction center (DI_O/RC).

Supplementary Files

This is a list of supplementary files associated with this preprint. Click to download.

- Supplement.docx